Dynamics of Polymer Blends with Intermolecular Hydrogen Bonding: Broad-Band Dielectric Study of Blends of Poly(4-vinyl phenol) with Poly(vinyl acetate) and EVA70

Shihai Zhang, Paul C. Painter, and James Runt*

Department of Materials Science and Engineering and Materials Research Institute, The Pennsylvania State University, University Park, Pennsylvania 16802

Received June 27, 2002

ABSTRACT: Strong intermolecular hydrogen bonding is capable of suppressing concentration fluctuations and coupling segmental relaxations in polymer blends whose components exhibit a large difference in their respective T_g's (ΔT_g). In this paper we report on our dielectric study of blends of poly(4-vinylphenol) [PVPh] with poly(vinyl acetate) [PVAc] and a random ethylene−vinyl acetate copolymer [EVA70]. Dielectric spectra were collected over a broad frequency range (0.01 Hz−10 MHz) for blends with PVPh concentrations ranging from 10% to 40%. Although both blends have large ΔT_g's (i.e., 116 K for PVPh/PVAc and 173 K for PVPh/EVA70), a single segmental relaxation was observed in most samples. This is attributed to the strong coupling arising from intermolecular hydrogen bonding. The fragility increases modestly with PVPh concentration as a result of enhanced intermolecular coupling. The effect of hydrogen bonding on fragility is discussed by considering hydrogen bond strength, its change with temperature, and competition between inter- and intramolecular association. Concentration fluctuations in PVPh/PVAc blends are insignificant, although PVPh/EVA70 blends show a broad relaxation time distribution as a result of their very large ΔT_g and the distribution of intermolecular hydrogen bonds. Some independently relaxing segments may involve only one intermolecular hydrogen bond, whereas others include two or more. The present results are also compared with those from our previous studies of PVPh/poly(ethyl methacrylate) and PVPh/poly(vinyl ethyl ether) blends.

Introduction

The properties of polymer blends can be tailored through selection of different components and by employing various processing methods. Polymer−polymer miscibility clearly plays a critical role in determining the final properties of such systems. One way of achieving enhanced miscibility is through the introduction of strong intermolecular interactions, e.g., hydrogen bonding.[1] Although the miscibility of polymer blends with intercomponent hydrogen bonding has been extensively studied using spectroscopic and other experimental methods, there has been relatively little research on their dynamical behavior.[2−6] Understanding the dynamics of polymer blends is important not only for property optimization but also for proper material processing.

For miscible polymer blends without strong interactions, two observations have generally been made in dielectric relaxation spectroscopy (DRS) or dynamic mechanical analysis (DMA) studies. First, for binary blends with relatively small T_g difference between their components (ΔT_g), i.e., $\Delta T_g \leq 50$ K, a single segmental (α) relaxation process is usually observed, with its relaxation time (τ) located between those of the two components at the same temperature. However, this relaxation process is usually very broad due to concentration fluctuations (CF), which are intrinsic to polymer blends. The breadth of the α relaxation time distribution increases with increasing concentration of the high-T_g component, if both components are dielectrically active, similar to the broadening of the DSC glass transition.[7,8] Concentration fluctuations in these blends have been successfully modeled by assuming a Gaussian distribution of local compositions in a cooperatively rearranging region (CRR), which in turn leads to a broadening of the relaxation time distribution.[9,10] However, it is worth noting that this model assumes that different CRRs have the same size, which is determined by the global T_g.

Second, the correlation between a single calorimetric T_g and a single DRS segmental relaxation process does not necessarily hold for blends with $\Delta T_g \geq 50$ K that do not have strong intermolecular interactions, due to the effect of concentration fluctuations and the intrinsic mobility difference between components.[11−14] Large-scale concentration fluctuations will likely occur in these thermodynamically complex blends, and two segmental relaxations can be observed, even though only the low-T_g component is dielectrically active: The fast process is attributed to the relaxation of the low-T_g polymer in an environment rich in itself, whereas the slow relaxation process stems from the low-T_g polymer in the blended environment. This has been confirmed by a dielectric study on polystyrene/poly(vinyl methyl ether) (PS/PVME, $\Delta T_g \approx 130$ K)[11] and was explained by a self-consistent concentration fluctuation model,[12] which modified the CRR concept in ref 9 by assuming that the size of the cooperatively rearranging regions changes with the local composition. Different compositions in different nanodomains lead to different local T_g's, and the size of the cooperatively rearranging regions is scaled by the temperature distance from its local T_g. Moreover, a large T_g contrast indicates large mobility differences, and it is possible that two calorimetrically miscible polymers relax individually with significantly different rates. Two segmental α relaxation processes have been clearly observed in poly(2-chlorostyrene)

* To whom correspondence should be addressed: e-mail runt@matse.psu.edu; phone 1-814-863-2749; fax 1-814-865-0016.

10.1021/ma021010i CCC: $22.00
Published on Web 9/21/2002

Table 1. Comparison of Intermolecular Hydrogen Bond Strengths of Selected PVPh Blends

	ΔT_g (K)	$-\Delta H^a$ (kcal/mol)	Δv^b (cm^{-1})	ref
PVPh/PVPh		5.2−5.4	155	15, 16
PVPh/PEMA	97	3.8		17
PVPh/PVAc	116	4.0		18
PVPh/EVA70	173	3.8		19
PVPh/PVEE	186	5.4	200	15

[a] Enthalpy of hydrogen bonding. [b] Wavenumber shift of hydrogen-bonded PVPh hydroxyl stretching mode from that of the free phenolic hydroxyl groups. Larger Δv indicates stronger hydrogen bonding.

[P2CS]/PVME blends ($\Delta T_g \approx 154$ K) and polyisoprene/poly(vinylethylene) [PIP/PVE] blends ($\Delta T_g \approx 60$ K), although a single calorimetric T_g was found in each case.[13,14]

Recently, we have studied the dynamics of hydrogen-bonded blends of poly(4-vinylphenol) [PVPh] with two proton-acceptor polymers using broad-band DRS, whose miscibility were confirmed by FTIR and DSC experiments. In a study of PVPh/poly(ethyl methacrylate) [PEMA] blends,[6] two prominent features were found. First, a single α relaxation process was observed, although ΔT_g of this blend is ∼97 K. Second, the segmental relaxation time distribution of the PVPh/PEMA blend is only marginally broader than neat PEMA, indicating that concentration fluctuations are suppressed. This was attributed to the effect of intermolecular hydrogen bonding, as predicted by the CF model described in ref 12. More striking relaxation behavior was observed, however, for the first time in our study of PVPh/poly(vinyl ethyl ether) [PVEE] blends.[15] The T_g difference between PVPh and PVEE is extremely large, i.e., ∼186 K, indicating a huge intrinsic mobility difference. Two separate segmental relaxations would be expected if there were no strong intermolecular hydrogen bonding, since the chemical structures of the components are very similar to P2CS/PVME and PS/PVME. However, two relaxations were only observed in blends with PVPh concentrations ≤20%. The slow process was attributed to the relaxation of hydrogen-bonded PVEE and PVPh segments and the fast one to "free" (nonassociated) PVEE segments. For blends ≥30% PVPh, a single α relaxation was observed, since essentially all PVEE segments are hydrogen-bonded with PVPh at these concentrations. This unusual relaxation behavior was explained in terms of the stoichiometry of intermolecular hydrogen bonding, and it was concluded that the hydrogen bond between PVPh and PVEE is capable of coupling the component segmental relaxations, which otherwise would relax individually.

In the present study, we report on our DRS study on blends of PVPh with two other polymeric proton acceptors, i.e., poly(vinyl acetate) [PVAc] and an ethylene−vinyl acetate random copolymer [EVA70, with 70 wt % vinyl acetate content]. Results of previous FTIR studies have shown that intermolecular hydrogen bonding in these blends is somewhat stronger than in PEMA/PVPh blends but clearly weaker than that in PVPh/PVEE mixtures. While the strength (enthalpy) of hydrogen bonds between PVPh and PVAc is the same as that between PVPh and EVA70, ΔT_g is ∼116 K for the former and ∼173 K for latter (see Table 1).[15−19] Following from the discussion above, ΔT_g and the strength of intermolecular interactions have an opposite effect on the segmental relaxations. Accordingly, the results from PVPh/PVAc and PVPh/EVA70 blends can be directly used to examine our previous conclusions concerning the influence of ΔT_g and intermolecular hydrogen bonding on segmental relaxations. Although the segmental relaxation of PVAc/PVPh has been studied by Luengo and co-workers using DMA and dynamic light scattering,[5] it was only performed for a blend with 20% PVAc concentration in a limited frequency range (0.1−30 Hz). Here we report a systematic study in a broad frequency window (0.01 Hz−10 MHz) with PVPh concentrations ranging from 10% to 40%. We focus on the effect of hydrogen bonding and ΔT_g on concentration fluctuations and intermolecular coupling. The present results will be compared with those previously obtained on PVPh/PVEE and PVPh/PEMA blends.

Experimental Section

A. Materials and Sample Preparation. PVPh and PVAc were purchased from Polysciences, Inc., with M_w of 41 000 and 121 000, respectively. EVA70 was the product of Scientific Polymer Products, Inc., with M_w = 441 000. The molecular weight distributions M_w/M_n for PVPh, PVAc, and EVA70 are 6.8, 5.1, and 7.2, respectively. Molecular weights were determined by gel permeation chromatography using narrow molecular weight poly(ethylene oxide) standards and dimethylformamide as the mobile phase. All polymers are used as received.

Blends with PVPh concentrations ranging from 10 to 40 wt % in 10% increments were prepared by casting from 5 wt % solutions of the component polymers in methyl ethyl ketone. The blends are designated as VV10−VV40 and VA10−VA40, where the number denotes the weight percentage of PVPh in the blend, VV refers to PVPh/PVAc blends, and VA refers to PVPh/EVA70 blends. The mixed solutions were stirred for at least 30 min before being cast onto Teflon-coated foil dishes. The solvent was removed in a vacuum oven by gradually increasing temperature to ∼20 K above T_g for at least 1 week. The neat PVAc and EVA70 films were prepared using the same method. All films were 0.1−0.2 mm thick. For DRS studies, gold was sputtered on both sides of the samples in an argon atmosphere. The films were kept in a vacuum desiccator prior to measurement. Because of the strong dc conductivity of PVPh, the α process in blends with more than 40% PVPh cannot be reliably resolved.

B. DRS Experiments. Dielectric relaxation spectra $\epsilon^*(f,T)$ were recorded isothermally using a Novocontrol GmbH Concept 40 broad-band dielectric spectrometer in the frequency domain [0.01 Hz−10 MHz] on cooling from T_g + 60 K to T_g. Sample films were sandwiched between two parallel gold-sputtered steel electrodes having a diameter of 20 mm. Temperature was controlled by a Novocontrol Quatro Cryosystem, which uses N_2 to heat and cool the sample and has a stability better than ±0.1 K.

C. DSC. Samples for DSC were cut directly from those prepared for DRS experiments. Glass transitions were studied using a Seiko SSC5200 instrument, which was calibrated by pure indium, with sample weights around 10 mg. The samples were first heated to ∼50 K above the expected T_g, held for 3 min, and then cooled at 20 K/min. After soaking at a minimum temperature (T_g − 40 K) for 5 min, the sample was heated again at a rate of 10 K/min. T_g was taken as the midpoint of the heat capacity change in the second heating run. Each sample was measured three times, and the average value is reported.

Results and Discussion

A. Blend Miscibility. According to the association model, PVPh and EVA copolymers are miscible if the vinyl acetate content in EVA is greater than 45%; this has been confirmed in previous FTIR and DSC studies.[1,19]

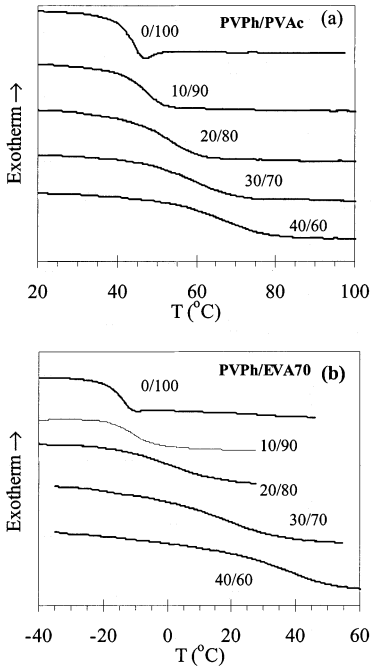

Figure 1. DSC thermograms of (a) PVPh/PVAc and (b) PVPh/EVA70. Taken from the second heating run with a heating rate of 10 K/min.

To facilitate comparison of segmental relaxations and glass transitions, we present the DSC traces in Figure 1. A single T_g is observed for each blend, confirming miscibility. However, the glass transition is substantially broadened in the blends as compared to those of the component polymers, indicating some degree of heterogeneity. Furthermore, PVPh/EVA70 blends have broader glass transition intervals than PVPh/PVAc blends. Broadening of the glass transition is generally observed in miscible blends and is attributed to both concentration fluctuations and differences in component mobility.[8] This behavior will be compared with similar DRS spectral broadening, since they have the same origin.

B. Dielectric Relaxation of PVPh/PVAc Blends. The dielectric relaxation behavior of PVAc has been studied by several research groups.[5,20−22] As usually observed in other homopolymers, segmental relaxation in PVAc occurs above the T_g and is slightly broader at high frequencies (Figure 2a). The peak shifts to higher frequency with increasing temperature as a consequence of faster relaxation. The segmental relaxation is a non-Arrhenius process, and its relaxation time, τ, follows the Vogel−Fulcher−Tammann (VFT) equation:[23]

$$\tau = \tau_0 \exp[B/(T - T_v)] \quad (1)$$

in which τ_0, B, and T_v are fitting parameters. τ_0 is the relaxation time at very high temperature, B is related to the apparent activation energy, and T_v is the Vogel temperature where the segments become immobile.

The dynamic relaxation process is usually described with the phenomenological Havriliak−Negami (HN) equation:[24]

$$\epsilon^*(\omega) = \epsilon'(\omega) - i\epsilon''(\omega) = \epsilon_\infty - i\frac{\sigma_0}{(\epsilon_v\omega)^s} + \frac{\Delta\epsilon}{[1 + (i\tau_{HN}\omega)^m]^n} \quad (2)$$

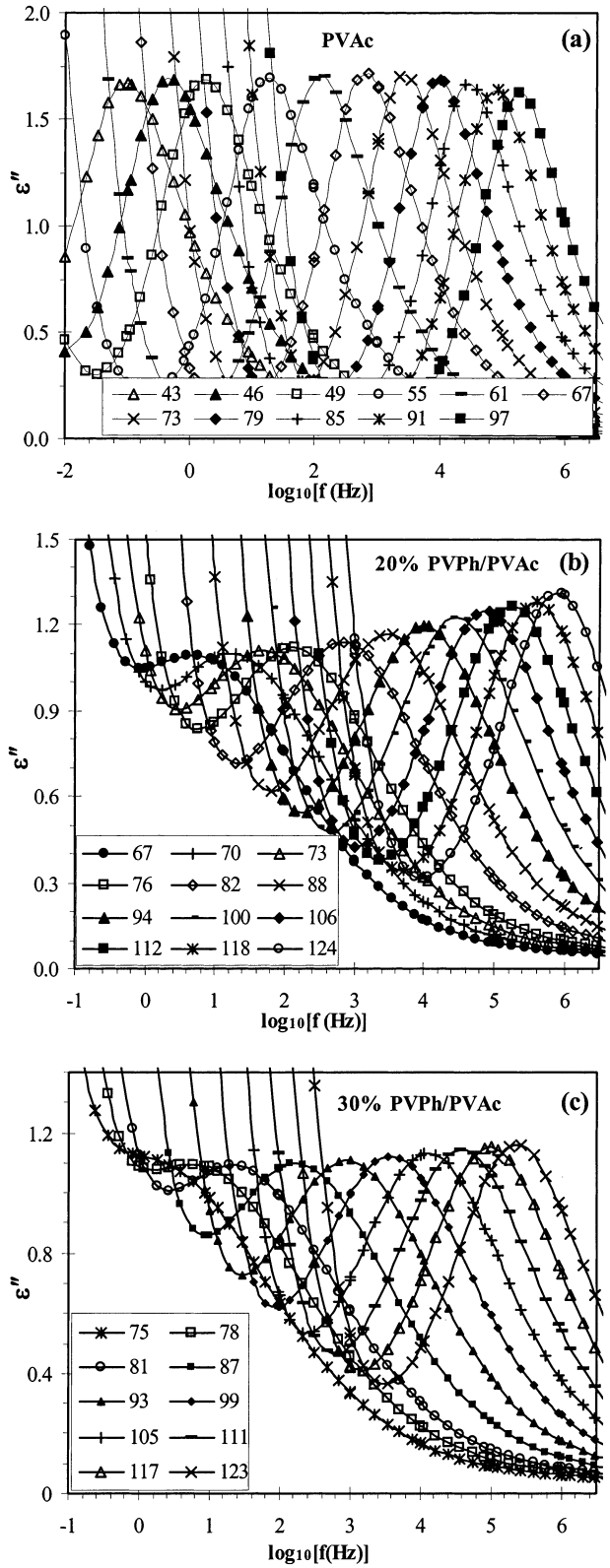

Figure 2. DRS loss spectra of (a) neat PVAc, (b) 20/80, and (c) 30/70 PVPh/PVAc blends. For clarity, only spectra at representative temperatures are shown. The upturn at low frequency is from dc conduction. Temperatures in °C.

Here $\omega = 2\pi f$, ϵ_∞ and ϵ_R are the unrelaxed and relaxed dielectric constant (ϵ') at very high and low frequency, respectively, and $\Delta\epsilon = \epsilon_\infty - \epsilon_R$ is the relaxation strength. ϵ_v is the vacuum permittivity. The exponents m and n ($0 < m$, $mn \leq 1$) are shape constants. σ_0 is the dc conduction constant with units of S/cm; the exponent s

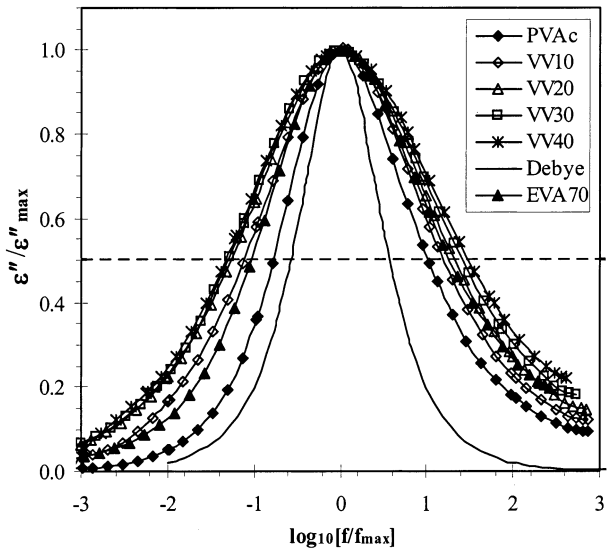

Figure 3. Normalized DRS loss spectra of PVPh/PVAc blends at $\sim T_{ref} + 35$ K. T_{ref}'s are defined as $\tau_{max}(T_{ref}) = 1$ s and are shown in Table 3. The dc conduction has been removed.

($0 < s \leq 1$) characterizes the conduction process. σ_0, s, τ_{HN}, $\Delta\epsilon$, m, and n are free variables in fitting the DRS loss spectra, ϵ''. τ_{HN} is related to the peak location τ_{max} by[25]

$$\tau_{max} = \tau_{HN}\left[\sin\frac{\pi mn}{2(n+1)}/\sin\frac{\pi m}{2(n+1)}\right]^{1/m} \qquad (3)$$

After using the HN function to obtain the relaxation times at different temperatures, we then fit $\tau_{max} - T$ with the VFT function. The fitted VFT parameters τ_0, B, and T_v for PVAc are 5×10^{-13} s, 0.135 eV, and 262 K, respectively. These values are similar to those reported by Yada and co-workers.[22]

Both PVPh and PVAc are dielectrically active with comparable dipole moments. The dipole moment of *p*-ethylphenol, a model for PVPh, is ~1.6 D. It is ~1.8 D for ethyl acetate, a small molecule analogue of the PVAc repeat unit.[26] Thus, the DRS relaxation includes contributions from both components. However, we observe a single segmental relaxation process for each composition at temperatures above their corresponding T_g's. For brevity, only DRS spectra of VV20 and VV30 at representative temperatures are shown in Figure 2. These data agree well with the DSC results and exclude large-scale concentration fluctuations (as observed for PVME/PS, PIP/PVE, and PVME/P2CS blends) and the existence of segments with large mobility differences. The ΔT_g of PVPh/PVAc is relatively small (i.e., ~116 K) compared with those of PVPh/PVEE blends (~186 K); the corresponding difference in mobility may not be sufficiently large to manifest itself as two separated segmental relaxation processes. A single α relaxation was also observed by Luengo et al. in their DMA study on a 20% PVPh/PVAc blend.[5]

Comparison of the segmental relaxation of blends with different compositions reveals that there are slight concentration fluctuations in the blends (Figure 3). The full width at half-maximum (fwhm) of the α relaxations increase with PVPh content. As discussed earlier, concentration fluctuations are a general characteristic of polymer blends. Different nanodomains (or cooperatively rearranging regions) have different compositions, each of which has a distinct T_g and thus different relaxation times, explaining the broadening of both the glass transition and the segmental relaxation.

Table 2. Full Width at Half-Maximum (fwhm) of the Dielectric Segmental Relaxations of Intermolecularly Hydrogen-Bonded Polymer Blends at Different Temperatures[a]

	PVAc	VV10	VV20	VV30	VV40
$T_{ref} + 35$ K	1.8	2.3	2.6	2.7	2.8
relative breadth[b]	1	1.3	1.4	1.5	1.6
$T_{ref} + 45$ K	1.7	2.2	2.4	2.5	2.6
relative breadth[b]	1	1.3	1.4	1.5	1.5
	EVA70	VA10	VA20	VA30	VA40
$T_{ref} + 25$ K	2.4	3.2	6.2	5.2	5.1
$T_{ref} + 35$ K	2.2	2.9	4.5	4.3	N/A
relative breadth[b]	1	1.3	2.1	2.0	N/A
	PEMA[c]	VE10	VE20	VE30	VE40
$T_{ref} + 45$ K	2.5	2.7	3.0	3.0	3.2
relative breadth[b]	1	1.1	1.2	1.2	1.3
	PVEE[d]	PE10	PE20	PE30	PE40
$T_{ref} + 30$ K	2.3	4.4	6.4	5.0	4.9
relative breadth[b]	1	1.9	2.8	2.2	2.1

[a] Units of the fwhm: decades, VV, VA, VE, and PE refer to the blends of PVPh with PVAc, EVA70, PEMA, and PVEE, respectively; the number after them denotes the weight percentage of PVPh in the blend. [b] Defined as the fwhm of the blend divided by the neat polymer. [c] PVPh/PEMA blends, from ref 6. [d] PVPh/PVEE blends, fwhm ≈5.0 for PE50, from ref 15.

However, according to the CF model detailed in ref 12, concentration fluctuations are predicted to be suppressed if there are strong intermolecular interactions, such as hydrogen bonding. For a 50/50 blend of poly(hexyl methacrylate) [PhMA] ($T_g = 268$ K) and poly(styrene-*co*-vinylphenol) [SHS50] ($T_g = 400$ K), these authors predicted that the distribution of local compositions in each CRR is sharply located around the overall blend concentration.[12] This was confirmed in our dielectric study of PVPh/PEMA blends.[6] Although PVPh/PVAc blends have a larger ΔT_g than PVPh/PEMA and concentration fluctuations are favored by a large T_g contrast, the hydrogen bonding between PVPh and PVAc is slightly stronger than that between PVPh and PEMA (Table 1). Thus, it is reasonable that concentration fluctuations in PVPh/PVAc are as insignificant as in PVPh/PEMA blends, as supported by comparison of their full width at half-maximum in Table 2, which show only a rather small increase with PVPh concentration. The relatively larger increase in fwhm of PVAc/PVPh compared with that of PVPh/PEMA blends is possibly a result of the comparatively broad molecular weight distribution of PVAc.

The minor segmental relaxation broadening in PVPh/PVAc blends is also seen in an isochronal plot of the dielectric constant at 1 kHz (Figure 4): blends containing higher concentrations of PVPh have slightly broader transition regions and higher transition temperatures. The transition in this plot contains similar information to the glass transition in the DSC experiment. In some particular temperature region, which is a function of the sweeping frequency, polymer chains gain significant mobility and the dipoles can be readily oriented; therefore, the dielectric constant exhibits a clear increase, just like the heat capacity jump in DSC.

The nominal dielectric spectrum broadening of PVPh/PVAc blends can also be a result of the distribution of intermolecular hydrogen bonds. As discussed for PVPh/

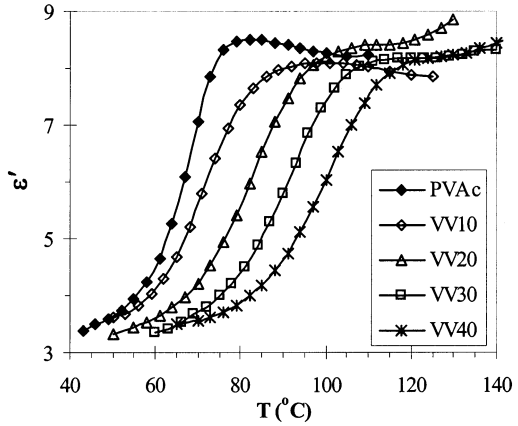

Figure 4. Isochronal plot of the dielectric constant ϵ' of PVPh/PVAc blends at 1 kHz.

PVEE blends,[15] intermolecular hydrogen bonding is a statistical process that is affected by chain connectivity effects.[27] Some independently relaxing segments (consisting of a number of chemical repeat units) may include one hydrogen bond, while others possibly involve two or more. These segments obviously have different relaxation times. In fact, this indicates heterogeneity at a segmental scale and can be regarded as "frozen" concentration fluctuations. This heterogeneity has a similar effect on the segmental relaxations as that resulting from concentration fluctuations but cannot change dynamically as rapidly as CF, due to constraint from intermolecular hydrogen bonds.

The blend becomes more homogeneous with increasing temperature as a result of reducing cooperative relaxation length scale; thus, the DRS spectra become narrower. On the other hand, the spectral breadth of neat PVAc is nearly independent of temperature, since there are no concentration fluctuations. This suggests that time−temperature superposition (TTS) should hold for PVAc but fail in the blends. This is the case, as shown in Figure 5. We have found that master dielectric loss curves can be obtained in 30−50% PVPh/PVEE blends due to the strong coupling between its two components.[15] The failure of TTS for PVPh/PVAc blends presumably results from the weaker intermolecular hydrogen bonds and broad molecular weight distributions in this system.

It is clear that the relaxation time increases with PVPh concentration, since the T_g of PVPh is much higher than that of PVAc (Figure 6a). To remove the T_g effect, we normalized the temperature using a reference temperature, T_{ref}, at which $\tau_{max} = 1$ s. The slope of log τ_{max} vs T_{ref}/T at $T_{ref}/T = 1$ is the so-called fragility F, as defined in eq 4:[28,29]

$$F = \left.\frac{\mathrm{d}\log \tau_{max}}{\mathrm{d}T_{ref}/T}\right|_{T=T_{ref}} \tag{4}$$

The fragility is a relative value and comparison between different materials is only meaningful if using a T_{ref} defined at the same relaxation time. It will be larger if a lower reference temperature corresponding to a longer relaxation time is used and smaller for a shorter τ_{max}.

Fragility is a measure of the ability of a material to change its conformation across the glass transition region. For polymers, it is also called "cooperativity"[30] and is usually correlated with the degree of intermolecular coupling. In Figure 6b, we observe an increase

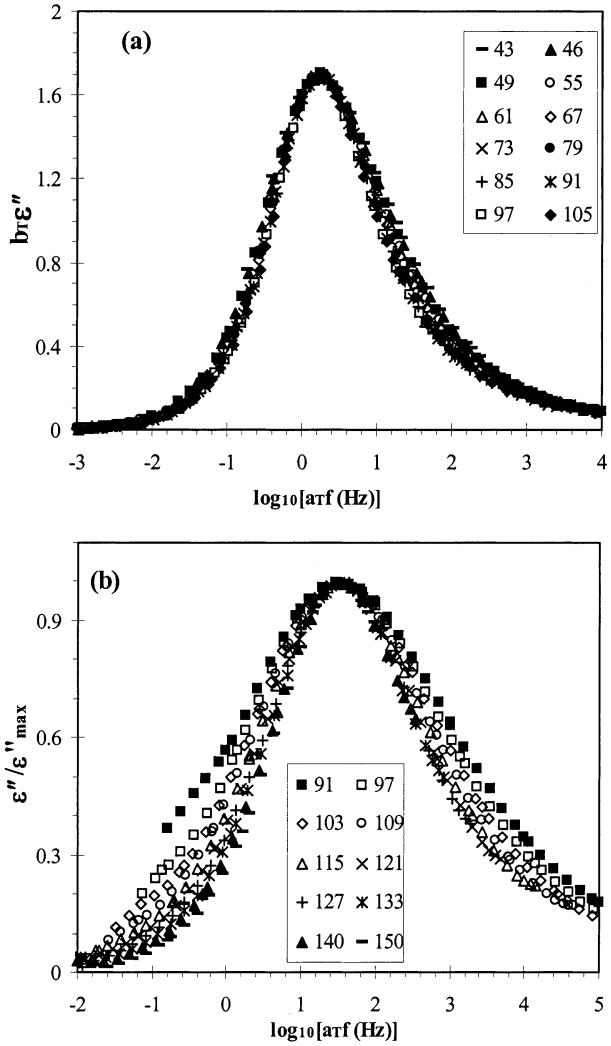

Figure 5. Temperature dependence of DRS loss spectra of (a) PVAc and (b) 40% PVPh/PVAc blend. Spectra have been shifted with respect to the spectrum shown as solid squares. The dc conduction has been removed.

in the slope with increasing PVPh concentration. Quantitatively, the fragility can be calculated from the VFT fitting parameters using eq 5:[31]

$$F = \frac{B/T_{ref}}{(\ln 10)(1 - T_v/T_{ref})^2} \tag{5}$$

However, it is often difficult to obtain reliable VFT parameters, since it is the points close to T_g that influence the regression most significantly, and it is usually hard to reliably obtain these dynamic data, because they require very long measurement times. Nevertheless, we are not interested in the physical precision of VFT parameters and the dynamic properties close to or below T_g but in the slope of the VFT plot at $T = T_{ref}$. Therefore, we reduced the number of free fitting variables by fixing $\tau_0 = 10^{-14}$ s. This is a reasonable assumption, since τ_0 is anticipated to have phonon-like time scales.[32] Using this method, the VFT regression is reproducible, and the fragility can be reliably calculated, even with only a few data points below T_{ref}. The fitted D and T_v values are listed in Table 3 along with the calculated T_{ref} and F. The fragility was found to increase from 66 for PVAc to 74 for the 40% blend, indicating that the cooperativity of the glass

Table 3. VFT Fitting Parameters, Reference Temperatures, and Fragility of the Blends[a]

	PVAc	VV10	VV20	VV30	VV40	EVA70	VA10	VA20	VA30	VA40
T_v[b] (K)	250.1	252.5	261.6	274.5	285.2	198.7	200.7	212.2	246.4	265.8
B[b](eV)	0.189	0.189	0.194	0.188	0.184	0.167	0.172	0.183	0.159	0.154
T_{ref}[c] (K)	318.0	320.6	331.5	342.2	351.6	258.6	262.5	278.0	303.6	321.1
F[d]	66	66	66	71	74	60	59	59	74	81

[a] VV refers to PVPh/PVAc blends and VA to PVPh/EVA70 blends; the number after VV or VA denotes the weight percentage of PVPh in the blend. [b] Fitted using the WinFit software from Novocontrol; τ_0 is fixed as 10^{-14} s. [c] Defined as $\tau_{max}(T_{ref}) = 1$ s. [d] Calculated using eq 5.

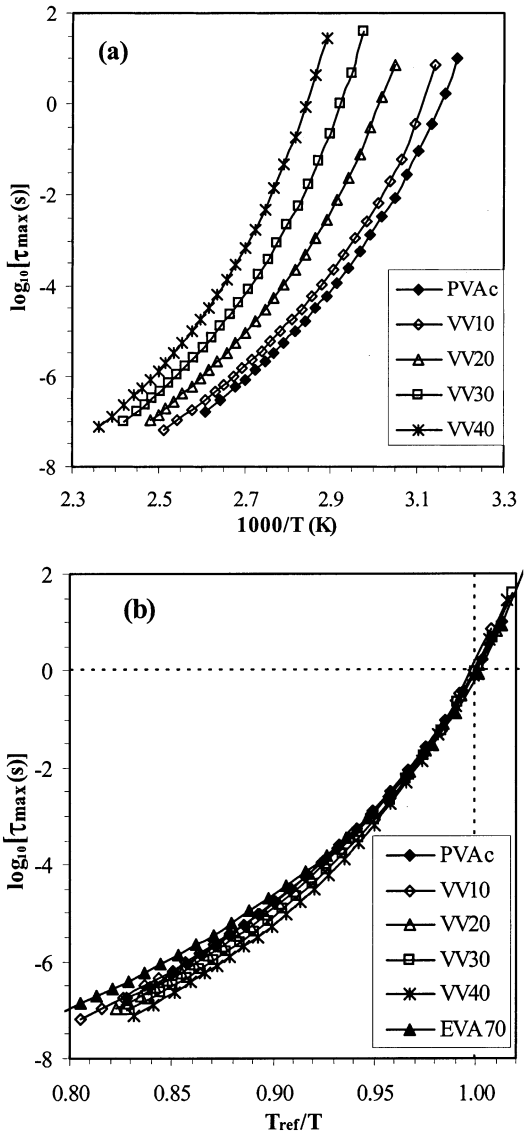

Figure 6. Relaxation time of PVPh/PVAc blend: (a) VFT plot and (b) fragility plot. T_{ref} is defined in Table 3.

transition and segmental relaxation is enhanced in the blends. Explained in a different way, considering the correlation between the fragility and the size of the cooperatively rearranging region,[33] the increase of fragility in PVPh/PVAc blends also indicates that the CRR size at the reference temperature becomes larger with increasing PVPh concentration, due to the coupling effect of intermolecular hydrogen bonding.

For polymers with weak intermolecular interactions, segmental mobility increases with temperature as a consequence of thermal activation and an increase in the free volume of the system: thus, the molecules are able to sample more conformations and the relaxation time decreases. If there is strong intermolecular hydrogen bonding, as in the PVPh/PVAc blends, and if the hydrogen-bonded fraction decreases with increasing temperature, a larger mobility increase can be expected, due to the additional freedom gained from the reduction in the average number of these strong, specific interactions. In other words, the decrease in the relaxation time is more rapid in the strongly interacting blends than in those without strong interactions. The forming and breaking of hydrogen bonds is a reversible process, and it shifts in the dissociated direction with increasing temperature; i.e., the equilibrium constant for hydrogen bonding becomes smaller.[1] This argument supports an increase of fragility in the PVPh/PVAc blends. However, we find the fragility increase to be very limited, as discussed below.

C. Segmental Relaxation of PVPh/EVA70 Blends. As an amorphous copolymer having a significant vinyl acetate content, EVA70 exhibits similar dielectric relaxation behavior to PVAc, since the ethylene repeat units are dielectrically inactive. Figure 7 presents the DRS loss spectra of EVA70 and the 40% PVPh/EVA70 blend. The relaxation time distribution of EVA70 is clearly broader than that of PVAc, with a full width at half-maximum of about 2.2 decades compared to 1.8 decades for PVAc at $T_{ref} + 35$ K. This is a consequence of copolymerization, which unavoidably introduces heterogeneity in monomer sequence distribution. As a result of increased T_g, the loss peaks in the PVPh/EVA70 blends are shifted to lower frequencies compared to neat EVA70.

Before discussing the dielectric relaxation behavior of PVPh/EVA70 blends, it is worth noting that the local β relaxation of PVPh occurs from −40 to 60 °C in the available frequency window, which overlaps with the segmental relaxation of the blends. Nevertheless, the relaxation strength of β(PVPh) is ∼10 times weaker than α(EVA70) due to its local nature (Figure 8); therefore, its influence on the segmental relaxations can be neglected when studying the latter.

The segmental relaxations in PVPh/EVA70 blends are more complicated than those in PVPh/PVAc blends. For the 30% and 40% blends, a single α process is clearly observed. For the 20% blend, however, there is a weak shoulder on the low-frequency side, which overlaps with both the dc conduction and the main α process. More surprisingly, the α peak of VA20 is even broader than that observed in VA30 and VA40, with fwhm of 6.2, 5.2, and 5.1 decades at $T_{ref} + 25$ K, respectively (Table 3). Although this behavior is different than that observed for the PVPh/PVAc blends, it is similar to the broadening behavior of PVPh/PVEE blends. The existence of two distinct segmental processes is reasonable, considering the large T_g contrast in PVPh/EVA70 blends and can be explained by the same stoichiometric effect proposed for PVPh/PVEE. That is, in 20% PVPh/EVA70 there are "free" EVA70 segments which relax faster and hydrogen-bonded segments whose relaxations are slower. For the 30% and 40% blends, all segments are hydrogen-bonded,

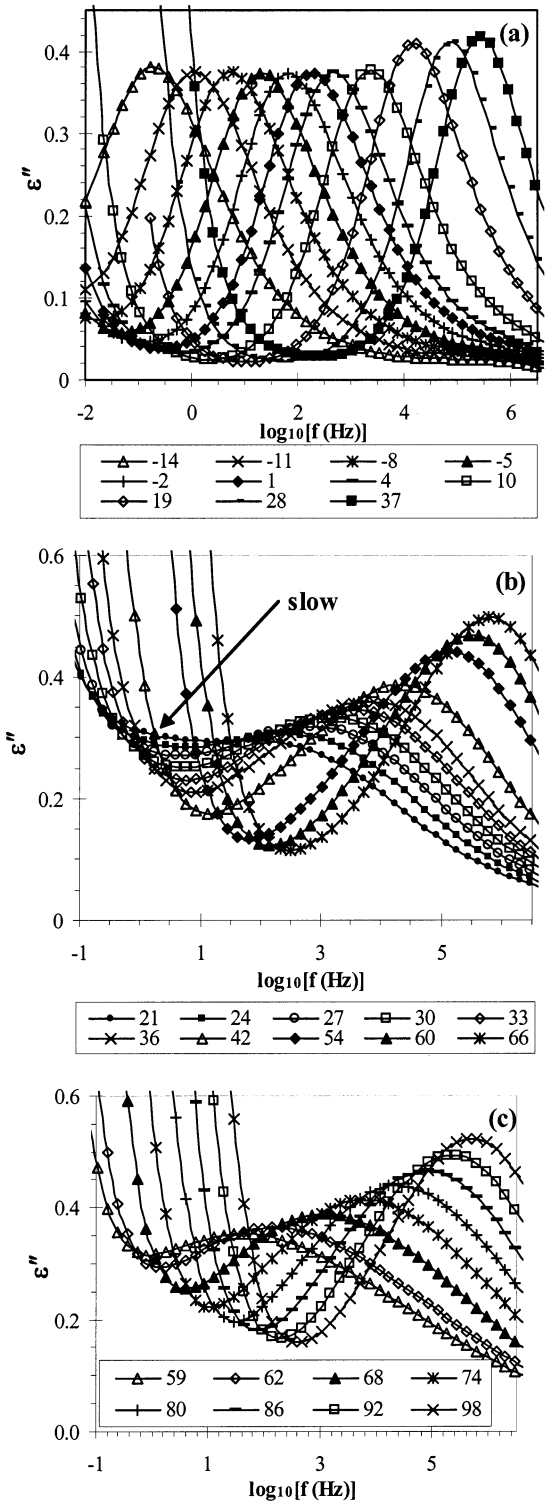

Figure 7. DRS loss spectra of (a) neat EVA70, (b) 20/80, and (c) 40/60 PVPh/EVA70 blends. For clarity, only spectra at representative temperatures are shown.

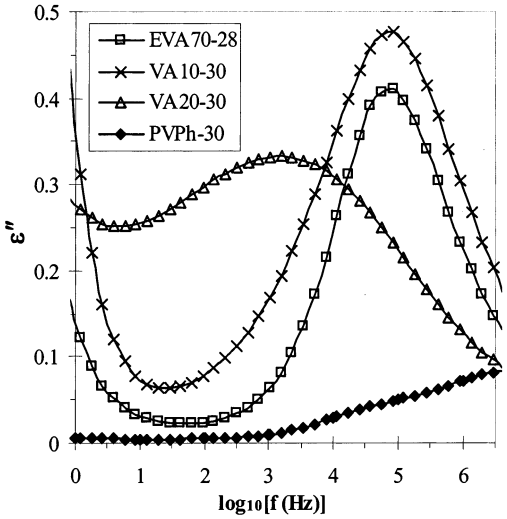

Figure 8. Comparing the β relaxation of PVPh and the segmental relaxations of PVPh/EVA70 blends. The number after the line denotes corresponding temperature in °C.

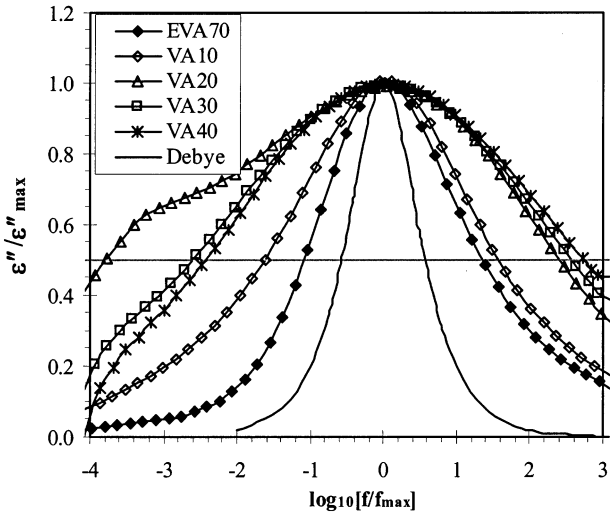

Figure 9. Normalized DRS loss spectra of PVPh/EVA70 blends at $\sim T_{ref}$ + 25 K. T_{ref}'s are defined as $\tau_{max}(T_{ref}) = 1$ s and are shown in Table 3. The dc conduction has been removed.

and hence a single α process is possible. However, we cannot quantitatively describe the slow process in the 20% blend, since it is too weak to be resolved using the general curve-fitting procedure.

Similar to neat EVA70, PVPh/EVA70 blends exhibit broad segmental relaxation time distributions compared to those of PVPh/PVAc blends (Table 2 and Figure 9). At a particular normalized temperature, i.e., T_{ref} + 35 K, the segmental relaxation time distribution of VA30 is almost 60% broader than for VV30. There is probably a ΔT_g effect in addition to the influence of copolymerization, as discussed above. Copolymerizing 30% ethylene into PVAc decreases the T_g to −15 °C, 55 °C lower than the homopolymer, and ΔT_g(PVPh/EVA70) is therefore 55 °C larger than ΔT_g(PVPh/PVAc). As discussed earlier, two phenomena are usually connected with large T_g contrast: concentration fluctuations and distinct component segmental relaxations. Concentration fluctuations are believed to be suppressed in intermolecularly hydrogen-bonded polymer blends and will not be considered here.[6,12] On the other hand, the very large ΔT_g for PVPh/EVA70 implies the existence of significant mobility difference between the two components. Although the two very different segmental relaxations can be coupled through intermolecular hydrogen bonding, this does not mean that they would relax with exactly the same rate, which is only possible in segments linked by chemical bonds. Hydrogen bonding couples the component relaxations by reducing, not necessarily eliminating, the differences. Considering the similar hydrogen-bonding strength in PVPh/EVA70 and PVPh/PVAc, the much larger ΔT_g in the former would be

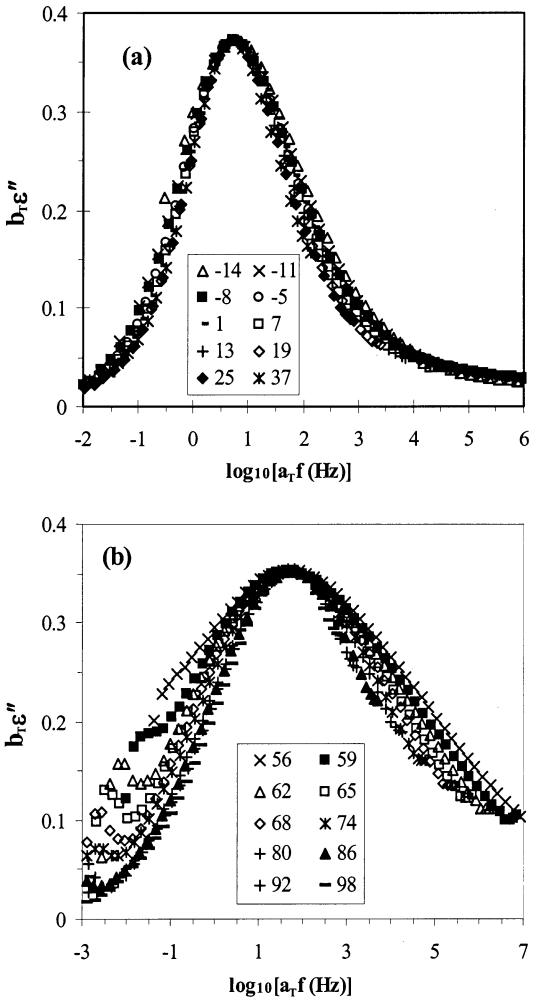

Figure 10. Temperature dependence of DRS loss spectra of (a) EVA70 and (b) 30% PVPh/EVA70 blend. Spectra have been shifted with respect to the spectrum shown as solid squares. The dc conduction has been removed.

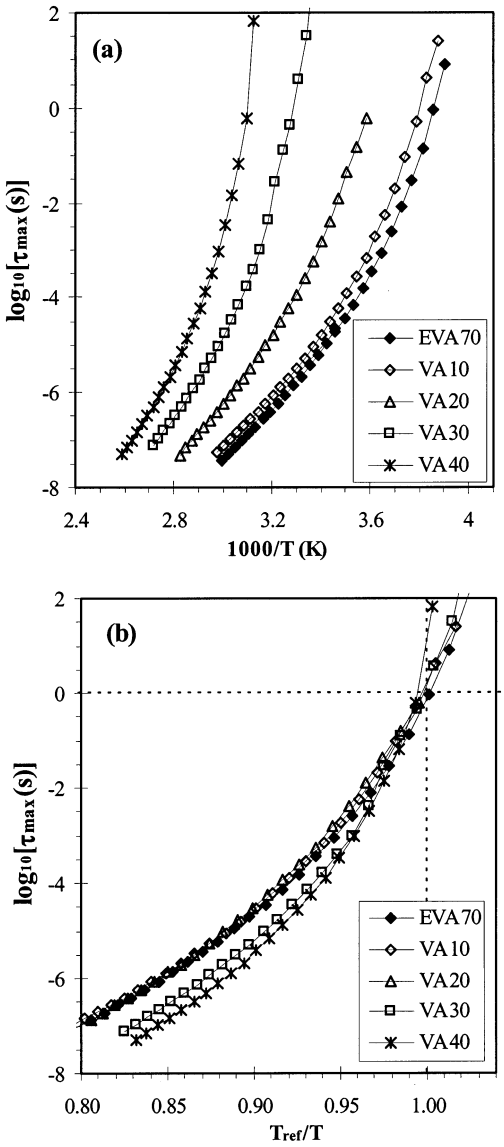

Figure 11. Relaxation time of PVPh/EVA70 blend: (a) VFT plot and (b) fragility plot. T_{ref} is defined in Table 3. For VA20 the relaxation times are from the main strong peak at higher frequency.

expected to lead to broader relaxation time distributions. The segmental relaxations of VA30 and VA40 have similar breadths, however, since all EVA70 segments have been hydrogen-bonded with PVPh.

The DRS loss spectra of PVPh/EVA70 blends become broader with decreasing temperature, whereas neat EVA70 has nearly the same fwhm at different temperatures (Figure 10). This is in agreement with the results observed for the PVPh/PVAc blends. Because of its lower T_g and the introduction of flexible ethylene units, EVA70 has a slightly lower fragility (60) than PVAc (66). Fragility of PVPh/EVA70 blends increases with PVPh concentration and can be explained using with the same argument as proposed earlier for PVPh/PVAc blends (Figure 11).

D. Effect of Hydrogen-Bonding Strength and ΔT_g. In the absence of concentration fluctuations, blends with a larger ΔT_g usually possess broader α relaxation peaks as a result of larger intrinsic mobility difference between the components. This is demonstrated in Table 2 by comparing blends of PVPh with different proton acceptors, i.e., PEMA,[6] PVAc, EVA70, and PVEE.[15] To remove the intrinsic broadening of the neat polymers, we define a relative peak breadth as the full width at half-maximum of the blend divided by that of the low-T_g polymer. It is found that the change in normalized relaxation breadth tracks with ΔT_g: PEMA < PVAc < EVA70 < PVEE, for 30% PVPh blends at a similar normalized temperature (Table 2).

A ΔT_g of 173 K for PVPh/EVA70 suggests that two separated dielectric segmental relaxation processes are expected if there are no strong intermolecular interactions, as in P2CS/PVME[13] and PIP/PVE.[14] Intermolecular hydrogen bonding between PVPh and EVA70 promotes homogeneity at the molecular level, reduces their mobility difference and coupling their segmental relaxations, as observed in PVPh/PVEE blends.[15] For PVPh/PVAc blends, ΔT_g is smaller, indicating a smaller mobility difference; thus, a single segmental relaxation is easier to achieve than in PVPh/EVA70 at the same hydrogen-bonding "strength".

The intriguing issue is, however, that the segmental relaxation separation behavior in PVPh/EVA70 blends was expected to be more evident than that in PVPh/PVEE blends, since the strength of intermolecular hydrogen bonding in the former is weaker than that in the latter and they have similar ΔT_g's (Table 1), indicating that the mobility differences between the components are comparable in the two mixtures. The weaker

intermolecular hydrogen bonds in PVPh/EVA70 blends suggest that the component segmental relaxations may not be coupled to the same extent as those in PVPh/PVEE blends. It is therefore possible that two separated α processes would be more clearly seen in the former. However, while we observe two distinct segmental relaxation processes for the 20% PVPh/PVEE blend, the DRS spectra of VA20 exhibits only moderate broadening, with a weak shoulder at low frequencies. This can be explained by considering the copolymerization effect in EVA70. The concentration of proton-acceptor groups in EVA70 is lower than in PVEE because of dilution from the ethylene repeat units. The mole ratio of −OH species to C═O in VA20 is about 25:100, while the −OH/-O− ratio in 20% PVPh/PVEE is about 15:100. This leads to a larger *fraction* of intermolecular hydrogen bonds per proton-acceptor group in the EVA70 system compared to the corresponding PVEE. As a consequence of the high −OH/C═O ratio, about 25% of the acetate groups are hydrogen-bonded with PVPh, according to a previous FTIR study.[19] The large fraction of intermolecular hydrogen bonds, following the same argument proposed for PVPh/PVEE blends,[15] suggests that all of the independent segments in PVPh/EVA70 will involve one or more hydrogen bonds, and their relaxations are thus coupled. In other words, the threshold concentration for PVPh to couple all of the component segmental relaxations is lower in the present blends than in PVPh/PVEE, and separated relaxation behavior is less apparent.

Finally, the fragility and intermolecular coupling in hydrogen-bonded blends deserve further comment. Coupling ability has been demonstrated by the observation of a single segmental relaxation process in blends with large ΔT_g and with sufficient intermolecular hydrogen bonds. However, since the strength of intermolecular hydrogen bonding between PVPh and PVAc (and EVA70) is weaker than that of self-association in PVPh (Table 1), this increase in intermolecular coupling is achieved at the expense of the decrease in intramolecular hydrogen bonds between PVPh segments. The observed segmental relaxation includes contributions from both components; therefore, the apparent coupling ability as assessed from DRS spectra represents a compromise between the decreased self-coupling of PVPh and the increased intermolecular coupling between PVPh and PVAc (or EVA70). Accordingly, the observed coupling in the blends is weaker than that expected from the enhanced cooperativity in the proton-acceptor component. Moreover, we argue that whereas higher fragility indicates stronger coupling, the reverse is only correct if the coupling can be significantly weakened with temperature. That is, it is the loss of coupling with increasing temperature, not the coupling strength itself, which influences the fragility. In PVPh/PVAc and PVPh/EVA70 blends, however, the hydrogen bond fraction does not change much with temperature.[19] For example, for the 20% PVPh/EVA70 blend, 25% of the acetate groups in EVA70 are hydrogen-bonded with PVPh, and this value is decreased only slightly (to 23%) as the temperature is increased to 80 °C higher. Therefore, the segments experience similar constraint from hydrogen bonding at different temperatures, and the change in their relaxation times is only influenced slightly by intermolecular hydrogen bonding. In fact, it has been proposed that only interactions with intermediate strength contribute to the fragility.[34] Strong interactions increase the barrier between different potential energy minima, and it is kinetically difficult for segments to sample different conformations. As a result, the fragility will not increase as thermodynamically expected.[28,29,35] Furthermore, it is worth pointing out that the fragility of neat PVPh may not be very high, compared to PVAc. Although it is not possible to dielectrically measure the fragility of PVPh, due to its strong dc conductivity, a study on styrene-*co*-vinylphenol copolymers found that the fragility does not change with composition (up to 18% VPh) and is ∼92 for different copolymers.[36] Since intermolecular coupling between acetate and PVPh is even weaker than the self-association in PVPh, the fragility of the blend cannot be higher than neat PVPh. Thus, the increase of fragility with PVPh concentration in these blends is not significant.

Summary

Segmental relaxations in polymer blends containing intermolecular hydrogen bonds were systematically investigated using broad-band dielectric relaxation spectroscopy. The miscibility of PVPh/PVAc and PVPh/EVA70 blends was confirmed by DSC. All PVPh/PVAc blends exhibit one segmental relaxation process, and their loss peaks are only broadened slightly as a consequence of strong intermolecular hydrogen bonding. For PVPh/EVA70 blends, however, two segmental relaxations are observed in the 20% blend, whereas other blend compositions exhibit one. This behavior is similar to that found in PVPh/PVEE blends and attributed to the large intrinsic mobility difference between the two components and an "insufficient" number of intermolecular hydrogen bonds to couple all segmental relaxations. Moreover, the segmental relaxation time distribution in PVPh/EVA70 is much broader than that for PVPh/PVAc blends, since the former have a ΔT_g that is 55 K larger than the latter. It was also found that the relative broadening of the different blends can be correlated with their ΔT_g's; i.e., a larger ΔT_g between the components correlates with enhanced broadening.

The fragility of both blends increases with increasing PVPh content due to enhanced intermolecular coupling. However, the increase is not large because of the loss of intramolecular hydrogen bonding in PVPh in the blend environment and the relatively small change in the fraction of hydrogen bonds with temperature.

Acknowledgment. The authors express their appreciation to the National Science Foundation, Polymers Program, for support of this research and the NSF-MRI program for support of the dielectric instrumentation (DMR-0079432).

References and Notes

(1) Coleman, M. M.; Graf, J. F.; Painter, P. C. *Specific Interactions and the Miscibility of Polymer Blends*; Technomic Publishing: Lancaster, PA, 1991.
(2) Sanchís, A.; Prolongo, M. G.; Masegosa, R. M.; Rubio, R. G. *Macromolecules* **1995**, *28*, 2693.
(3) Prolongo, M. G.; Salom, C.; Masegosa, R. M.; Moreno, S.; Rubio, R. G. *Polymer* **1997**, *38*, 5097.
(4) Li, D.; Brisson, J. *Macromolecules* **1996**, *29*, 868.
(5) Luengo, G.; Ortega, F.; Rubio, R. G.; Rey, A.; Prolongo, M. G.; Masegosa, R. M. *J. Chem. Phys.* **1994**, *100*, 3258.
(6) Zhang, S. H.; Jin, X.; Painter, P. C.; Runt, J. *Macromolecules* **2002**, *35*, 3636.
(7) Runt, J. P. In *Dielectric Spectroscopy of Polymeric Materials*; Runt, J. P., Fitzgerald, J. J., Eds.; American Chemical Society: Washington, DC, 1997; Chapter 10.

(8) Lodge, T. P.; McLeish, T. C. B. *Macromolecules* **2000**, *33*, 5278.
(9) Zetsche, A.; Fisher, E. W. *Acta Polym.* **1994**, *45*, 168.
(10) Katana, G.; Fischer, E. W.; Hack, T.; Abetz, V.; Kremer, F. *Macromolecules* **1995**, *28*, 2714.
(11) Pathak, J. A.; Colby, R. H.; Floudas, G.; Jérôme, R. *Macromolecules* **1999**, *32*, 2553.
(12) Kumar, S. K.; Colby, R. H.; Anastasiadis, S. H.; Fytas, G. *J. Chem. Phys.* **1996**, *105*, 3777.
(13) Urakawa, O.; Fuse, Y.; Hori, H.; Tran-Cong, Q.; Yano, O. *Polymer* **2001**, *42*, 765.
(14) Arbe, A.; Alegría, A.; Colmenero, J.; Hoffmann, S.; Willner, L.; Richter, D. *Macromolecules* **1999**, *32*, 7572.
(15) Zhang, S. H.; Painter, P. C.; Runt, J. *Macromolecules*, in press.
(16) Moskala, E. J.; Varnell, D. F.; Coleman, M. M. *Polymer* **1985**, *26*, 228.
(17) Serman, C. J.; Xu, Y.; Painter, P. C.; Coleman, M. M. *Polymer* **1991**, *32*, 516.
(18) Zhang, H. X.; Bhagwagar, D. E.; Graf, J. F.; Painter, P. C.; Coleman, M. M. *Polymer* **1994**, *35*, 5379.
(19) Xu, Y.; Painter, P. C.; Coleman, M. M. *Makromol. Chem., Macromol. Symp.* **1991**, *52*, 91.
(20) Smith, G. D.; Boyd, R. H. *Macromolecules* **1991**, *24*, 2731.
(21) Smith, G. D.; Liu, F. G.; Devereaux, R. W.; Boyd, R. H. *Macromolecules* **1992**, *25*, 703.
(22) Yada, M.; Nakazawa, M.; Urakawa, O.; Morishima, Y.; Adachi, K. *Macromolecules* **2000**, *33*, 3368.
(23) Ferry, J. D. *Viscoelastic Properties of Polymers*; Wiley: New York, 1980.
(24) Havriliak, S.; Negami, S. *J. Polym. Sci., Polym. Symp.* **1966**, *14*, 99.
(25) Havriliak, S.; Havriliak, S. J. In *Dielectric Spectroscopy of Polymeric Materials*; Runt, J. P., Fitzgerald, J. J., Eds.; American Chemical Society: Washington, DC, 1997; Chapter 6.
(26) McClellan, A. L. *Tables of Experimental Dipole Moments*; Rahara Enterprises: El Cerrito, CA, 1974.
(27) Painter, P. C.; Veytsman, S.; Kumar, S.; Graf, J. F.; Xu, Y.; Coleman, M. M. *Macromolecules* **1997**, *30*, 932.
(28) Angell, C. A. *J. Non-Cryst. Solids* **1991**, *131*−*133*, 13.
(29) Angell, C. A. *Science* **1995**, *267*, 1924.
(30) Roland, C. M.; Ngai, K. L. *Macromolecules* **1991**, *24*, 5315.
(31) Hodge, I. M. *J. Non-Cryst. Solids* **1996**, *202*, 164.
(32) Angell, C. A. *Polymer* **1997**, *38*, 6261.
(33) Erwin, B. M.; Colby, R. H. *J. Non-Cryst. Solids* **2002**, *225*, 307−310.
(34) Santangelo, P. G.; Roland, C. M. *Macromolecules* **1998**, *31*, 4581.
(35) Roland, C. M.; Santangelo, P. G.; Ngai, K. L. *J. Chem. Phys.* **1999**, *111*, 5593.
(36) Schroeder, M. J.; Roland, C. M.; Kwei, T. K. *Macromolecules* **1999**, *32*, 6249.

MA021010I